Identifying a Non-Maneuvering Warhead Separation From a Reentry Vehicle in Cluttered Environments

Cheng-Yu Liu* and Yu -Ming Sung

Department of Electronic Engineering, Lee-Ming Institute of Technology.

ABSTRACT

Monitoring a warhead between two objects separated from a reentry vehicle in a clear environment has recently become an important issue. However, clutter, caused by the sea, land, clouds, and weather, are unavoidable and degrade tracking performance. The Hough transform is an effective means of identifying a straight line in a noisy environment. This study presents a novel tracking filter that integrates a target acquisition algorithm and an accurate identification method for identifying a non-maneuvering warhead among more than two objects separated from a reentry vehicle in a cluttered environment. The target acquisition algorithm, based on the Hough transform, selects two candidates from detected objects and clutter. The identification method, comprising an extended Kalman filter with input estimation and modified probabilistic data association filter, provides a good tracking capability for a warhead from two candidates selected by the target acquisition algorithm. Simulation results reveal that estimation errors of warhead trajectory are reduced to a small interval within a short time. Therefore, radar can track a warhead all the time from one search. We conclude that this algorithm is worthy of further study and application.

Keywords: reentry vehicle, input estimation, Hough transform, modified probabilistic data association filter

於雜波環境下鑑識分裂自重返載具之無操縱性彈頭法則

劉正瑜*　宋馭民

黎明技術學院電子系

摘　　要

在無雜波環境下，追蹤重返載具分裂為彈頭與彈體中之彈頭，是為相當重要之議題。然由海、陸地、氣候及其他因素所引起之雜波，會降低雷達之追蹤彈頭性能。Hough 轉換為於雜訊環境下，偵測直線之一有效方法。另由於技術之增進，重返載具已能同時分裂為超過兩個以上之物體，基此二因素，本論文旨在發展一以 Hough 轉換為基礎之目標鑑識法則，並結合擴展性 Kalman 濾波器與輸入估測，期能於雜訊環境下及多個分裂物體中，準確辨識無操縱性之彈頭，以維持雷達之穩定追蹤。此一鑑識法則將自含雜波在內之物體中，選擇兩個可能為彈頭之物體，送入修正之機率數據結合濾波器，應用擴展性 Kalman 濾波器與輸入估測，獲得彈頭之預估狀態，以供相列雷達產生波束鎖定彈頭。由模擬證明，低彈頭預估誤差，可保證雷達鎖定無誤。此一結果顯示本法則值得加以持續研究與應用。

關鍵詞：重返載具，輸入估測，Hough 轉換，修正之機率數據結合濾波器

文稿收件日期 98.5.17; 文稿修正後接受日期 99.3.5;*通訊作者
Manuscript received May 17 ,2009; revised March 5,2010 ;* Corresponding author

I. INTRODUCTION

Separating a reentry vehicle (RV) into several objects, including the warhead, main body and debris during the reentry phase, is an effective way of confusing radar by inducing many measurement sets. The body or debris is then tracked and intercepted first, since its radar cross section is inevitably larger than that of a warhead. Tracking a warhead, which is the most significant part of RV, becomes difficult when the traditional tracking algorithm is employed. Furthermore, clutter is unpredictable and unavoidable in radar tracking, and causes radar to randomly receive numerous echoes in one scan, thereby complicating the warhead identification problem. Seldom unclassified papers and tracking algorithms were dealing with this problem under cluttered environments for radar design. Two issues, estimation of warhead trajectory and origination of measurements, are resolved to solve this problem. On-line precision trajectory estimation approach and data association technique are required. This is the major concern for this paper.

Clutter is unwanted signal echoes from the sea, land, clouds, or weather. Numerous researchers have endeavored to study methods of clutter suppression by utilizing Doppler shift and moving target indicator addressed in hardware design [1]. Although effective, these approaches are extremely costly. Phased array radar has been a focus of design efforts during past two decades. Certain signal processing functions are accomplished via digital computers. Algorithm development then became the primary task in achieving desired tracking performance in cluttered environments. The Hough transform (HT) was designed for identifying straight lines in noisy environments and was applied to the tracking problems [2] and air traffic control [3]. If a warhead does not alter its trajectory after separation, then it generally follows the original trajectory closely. However, the vehicle body and debris deviate from the initial trajectory and clutter appears at random locations and in random directions. Thus, the HT is useful for identifying a non-maneuvering warhead by analyzing its straight fly path formed by the trajectories estimated at previous times and measured at present.

On-line estimation of RV or warhead trajectory is limited mainly with respect to model validation, due to model error between the mathematical model and the physical system. Model error generally results from simplifying assumptions, maneuvering and unpredictable external forces during flight or from parameter uncertainty. The extended Kalman filter (EKF) is a well-known state estimation scheme, but fails to rapidly achieve the required accuracy. Lee and Liu created a filter combining the EKF with input estimation to deal with model validation problems, and generated an accurate trajectory estimation approach for RVs in clear environments [4] and was widely applied [5,6].

Bar-Shalom designed the probabilistic data association filter for tracking a single target in cluttered environments [7,8,9,10]. A modified probabilistic data association filter (MPDAF) associating with the EKF and input estimation was developed for identifying warhead between two objects split from an RV in a clear environment [11]. This algorithm makes the warhead tracking under a complicated situation in which many objects and clutter are involved to be possible.

This study presents a novel and simple tracking algorithm to deal with issues this paper concerns. The proposed method comprises a target acquisition algorithm based on the Hough transform, EKF with input estimation, and MPDAF and enables radar to keep tracking the warhead following separation. The target acquisition algorithm is designed for selecting two candidates from measured objects and clutter. The EKF with input estimation provides accurate updated states for two candidates. The combined updated state is obtained by the developed MPDAF. Small errors between the combined state and warhead trajectory guarantee the warhead to be track well. Simulation results reveal that it is helpful to radar design.

The remainder of this paper is organized as follows. Section 2 presents a detailed problem statement that elucidates the problem, and formulates dynamic equations for all objects and clutter. Section 3 describes the target acquisition algorithm. Section 4 outlines the EKF algorithm with input estimation. Section 5 presents the MPDAF and detailed steps of the proposed algorithm to estimate and predict the warhead trajectory for tracking purposes. Section 6

summarizes simulation results of the proposed filter. Finally, conclusions are given in Section 7.

II. DYNAMIC EQUATIONS

Define the radar Cartesian coordinate system to be centered at the radar site O_R with three axes downrange X_R, offrange Y_R, and altitude Z_R. Figure 1 shows a vehicle in the reentry phase over a flat and non-rotating earth. Assume the RV is a point mass with constant weight following a ballistic trajectory in which two significant forces, drag and gravity, that act on the RV. Extra forces are induced by model error when assumptions are violated or the RV undertakes a maneuver. The RV trajectory model can be written as [4]

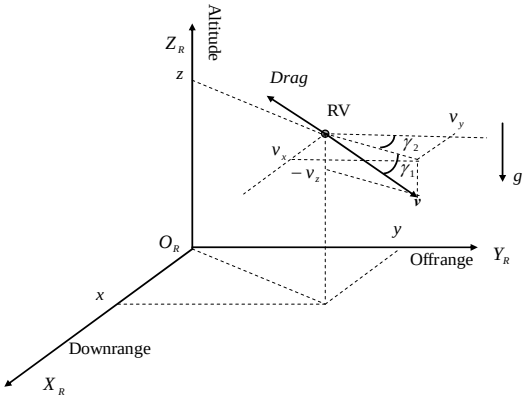

Fig. 1. Reentry Vehicle Flight Geometry.

$$\dot{v}_x = -\frac{\rho v^2}{2C} g \cos\gamma_1 \sin\gamma_2 + u_x \qquad (1)$$

$$\dot{v}_y = -\frac{\rho v^2}{2C} g \cos\gamma_1 \cos\gamma_2 + u_y \qquad (2)$$

$$\dot{v}_z = \frac{\rho v^2}{2C} g \sin\gamma_1 - g + u_z \qquad (3)$$

with position initial conditions $x(0)$, $y(0)$, $z(0)$ and velocity initial conditions $v_x(0)$, $v_y(0)$, and $v_z(0)$ in X_R, Y_R and Z_R, respectively. In this model, C denotes the ballistic coefficient,

$$C = \frac{W}{SC_{D0}}$$

$$\gamma_1 = \tan^{-1}\left(-\frac{v_z}{\sqrt{v_x^2 + v_y^2}}\right)$$

$$\gamma_2 = \tan^{-1}\left(\frac{v_x}{v_y}\right)$$

v is the total velocity of the RV, v_x, v_y, and v_z express velocity components along X_R, Y_R, and Z_R, respectively; u_x, u_y, and u_z are un-modeled accelerations generated by the model errors along each axis; C_{D0}, S and W denote zero-lift drag coefficient, reference area and, weight respectively. ρ stands for air density and is a function of altitude. The well known normal gravity g model is extensively used because the RV normally flies over heights of several hundred kilometers [12].

Let the state vector be

$$\boldsymbol{X}(t) = \begin{bmatrix} x_1 & x_2 & x_3 & x_4 & x_5 & x_6 \end{bmatrix}^T = \begin{bmatrix} x & y & z & v_x & v_y & v_z \end{bmatrix}^T \qquad (4)$$

The nonlinear state equation can be written as

$$\dot{\boldsymbol{X}}(t) = F(\boldsymbol{X}) + \varphi \boldsymbol{u} + \boldsymbol{\zeta} \qquad (5)$$

where

$$F(\boldsymbol{X}) = \begin{bmatrix} x_4 \\ x_5 \\ x_6 \\ -\frac{\rho}{2C_b}(x_4^2 + x_5^2 + x_6^2) g \cos\gamma_1 \sin\gamma_2 \\ -\frac{\rho}{2C_b}(x_4^2 + x_5^2 + x_6^2) g \cos\gamma_1 \cos\gamma_2 \\ \frac{\rho}{2C_b}(x_4^2 + x_5^2 + x_6^2) g \sin\gamma_1 - g \end{bmatrix}$$

$$\varphi = \begin{bmatrix} \boldsymbol{0}_{3\times3} & \boldsymbol{0}_{3\times3} \\ \boldsymbol{0}_{3\times3} & \boldsymbol{I}_{3\times3} \end{bmatrix}$$

$$\boldsymbol{u} = \begin{bmatrix} 0 & 0 & 0 & u_x & u_y & u_z \end{bmatrix}^T$$

$\boldsymbol{\zeta}$ denotes the process noise which is assumed to be normally distributed with mean zero and variance $\boldsymbol{Q}$, $\boldsymbol{0}_{3\times3}$ and $\boldsymbol{I}_{3\times3}$ are 3×3 dimensional zero and identity matrices.

The phased array radar with high resolution and precision is used in tracking, and is the only instrument in the system for detecting the RV. Assume the bias of the radar to be corrected before detection. The detected elevation, azimuth, and range are transferred into position. Since the detected velocity measured from pulse Doppler did not meet the accuracy needs, the velocity obtained by a specific filter in radar is taken as the measurements to improve estimation accuracy. If the filter is taken into account, a nonlinear measurement equation is involved and become too complicated to be accomplished. For simplicity and being easily implemented, the effects of nonlinearity induced by filtering are ignored. The linear measurement equation for the RV is then given by [4]

$$\boldsymbol{Z}(t) = \boldsymbol{X}(t) + \boldsymbol{\varepsilon}(t) \tag{6}$$

where $\boldsymbol{\varepsilon}$ denotes the measurement noise vector, which is assumed to be normally distributed with mean zero and variance $\boldsymbol{R}$. Equations (5) and (6) are the dynamic equations for the RV during reentry.

The radar predicts the target position at the next sampling period according to a set of measurements, and creates a search pattern to illuminate the predicted position to track the target. The phased array radar emits radar beams to form a certain search pattern centered at the predicted target position. Radius of a search pattern cross section is usually several times of radius of a beam cross section. Once the target locates outside the pattern, the radar will terminate the tracking procedure.

An RV separates into N_o objects, including the warhead, body and debris, at $t = t_s$. The body and debris then deviate from the original RV trajectory. Equations of motion for N_o objects with the ballistic coefficients C_i, $i = 1,2,\cdots,N_o$, after separation are given by

$$\dot{v}_{xi} = -\frac{\rho v_i^{\,2}}{2C_i} g \cos\gamma_{1i} \sin\gamma_{2i} + u_{xi} \tag{7}$$

$$\dot{v}_{yi} = -\frac{\rho v_i^{\,2}}{2C_i} g \cos\gamma_{1i} \cos\gamma_{2i} + u_{yi} \tag{8}$$

$$\dot{v}_{zi} = \frac{\rho v_i^{\,2}}{2C_i} g \sin\gamma_{1i} - g + u_{zi} \tag{9}$$

with position initial conditions $x_i(t_s)$, $y_i(t_s)$, $z_i(t_s)$ and velocity initial conditions $v_{xi}(t_s)$, $v_{yi}(t_s)$, and $v_{zi}(t_s)$ in X_R, Y_R and Z_R, respectively, v_i denotes the total velocity of the *i*-th object, γ_{1i} and γ_{2i} express the elevation and flight path angles, respectively; u_{xi}, u_{yi}, and u_{zi} are unpredictable input accelerations acting on the *i*-th object.

Let the state vector for the *i*-th object to be

$$\begin{aligned}\boldsymbol{X}_i(t) &= \begin{bmatrix} x_{1i} & x_{2i} & x_{3i} & x_{4i} & x_{5i} & x_{6i} \end{bmatrix}^{T\,T} \\ &= \begin{bmatrix} x_i & y_i & z_i & v_{xi} & v_{yi} & v_{zi} \end{bmatrix}^T \end{aligned} \tag{10}$$

The nonlinear state equation can be written as

$$\begin{aligned}\dot{\boldsymbol{X}}_i(t) &= F(\boldsymbol{X}_i) + \varphi \boldsymbol{u}_i + \boldsymbol{\zeta}_i \\ & \qquad i = 1,2,\cdots,N_o \quad t > t_s \end{aligned} \tag{11}$$

where ζ_i stands for the process noise vector applying to the *i*-th object with variance $\boldsymbol{Q}_i$,

$$\boldsymbol{u}_i = \begin{bmatrix} 0 & 0 & 0 & u_{xi} & u_{yi} & u_{zi} \end{bmatrix}^T$$

The measurement equation for the *i*-th object is then given by

$$\begin{aligned}\boldsymbol{Z}_i(t) &= \boldsymbol{X}_i(t) + \varepsilon'(t) \\ & \qquad i = 1,2,\cdots,N_o \quad t > t_s \end{aligned} \tag{12}$$

where ε' expresses the measurement noise vector the same as ε in Eq. (6).

Assuming that N_c clutter positions (x_i^c, y_i^c, z_i^c) and velocities $(v_{xi}^c, v_{yi}^c, v_{zi}^c)$, i=1, 2,…, N_c, are measured near the warhead of the RV in a search pattern after separation. The clutter number, N_c, and location are generally assumed to be Poisson and uniformly distributed, respectively [3].

Let the state vector, $\boldsymbol{X}_i^c(n)$, be comprised the position and velocity of the *i*-th clutter. Ignoring noise, the measurement equations are then given by

$$\boldsymbol{Z}_i^c(n) = \boldsymbol{X}_i^c(n) \qquad i = 1,2,...,N_c \tag{13}$$

Equations (12) and (13) are gathered $N = N_o + N_c$ measurement sets via one search. Clearly, if a clutter or an object but a warhead is

chosen from N sets, the radar loosens the warhead and tracks clutter, body, or debris. This serious problem should be solved to ensure track maintenance. To achieve tracking purpose, a precise trajectory estimation and an effective target acquisition algorithm are required.

III. TARGET ACQUISITION ALGORITHM

The main task of the proposed target acquisition algorithm is to select the set of warhead measurements from N measurement sets. It is too difficult and complicated to achieve this. The MPDAF was well defined and successfully applied to track the warhead between two separation objects. This filter provides an useful way to deal with the problem of set selection. This section defines an algorithm based on the HT to select two candidates from N objects after separation. These two candidates are sent into the EKF with IE and MPDAF to predict warhead states.

The HT was developed to identify straight lines in a noisy environment. Consider a point (x, y) in a Cartesian frame. This point can be transformed into the ρ-θ plane by following [2]

$$\rho = x\cos\theta + y\sin\theta \qquad 0 \le \theta \le \pi \qquad (14)$$

Various points in a Cartesian frame generate a family of curves in the ρ-θ plane. If n points, $(x_1, y_1), (x_2, y_2)$, …, (x_n, y_n), lie on a straight line, their transform have a common point. This feature helps in censoring some objects and clutter, whose trajectories deviate from the original, before identifying the warhead.

Let the sampling time is small enough such that the predicted warhead position can be assumed to be a straight line with two previous predicted positions after separation. Figure 2 demonstrates this concept. The measured quantities of the i-th objects, ($q_{ui}(n+1)$, $q_{vi}(n+1)$), and the i-th clutter, ($q_{ui}^c(n+1)$, $q_{vi}^c(n+1)$), in a certain two dimensional plane, u-v, at $t = (n+1)\Delta t$ are taken into account. The HT of objects and clutter are given by

$$\rho_i(n+1) = q_{ui}(n+1)\cos\theta + q_{vi}(n+1)\sin\theta \qquad i = 1,2,...N_o \qquad (15)$$

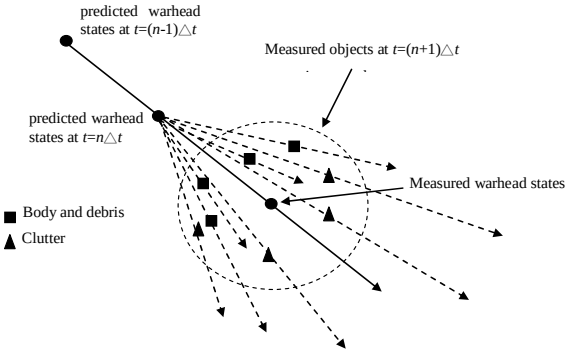

Fig. 2 Concept of target acquisition algorithm.

$$\rho_i^c(n+1) = q_{ui}^c(n+1)\cos\theta + q_{vi}^c(n+1)\sin\theta \qquad i = 1,2,...N_o \qquad (16)$$

The HT of two updated quantities in u-v plane, $(\hat{q}_u^v(n|n), \hat{q}_v^v(n|n))$ at $t = n\Delta t$ and $(\hat{q}_u^v(n-1|n-1), \hat{q}_v^v(n-1|n-1))$ at $t = (n-1)\Delta t$ can be written as

$$\rho(n) = \hat{q}_u^v(n|n)\cos\theta + \hat{q}_v^v(n|n)\sin\theta \qquad (17)$$

$$\rho(n-1) = \hat{q}_u^v(n-1|n-1)\cos\theta + \hat{q}_v^v(n-1|n-1)\sin\theta \qquad (18)$$

If the j-th quantity ($q_{uj}(n+1), q_{vj}(n+1)$) is the measurement of real track, the j-th equation in Eq. (15) shares a common point with Eqs. (17) and (18). If ($q_{uj}^c(n+1)$, $q_{vj}^c(n+1)$) is the measurement of real target, the corresponding equation in Eq. (16) intersects Eqs. (17) and (18) at a point.

Let the common point of Eqs. (17) and (18) are located at (ρ^*, θ^*). It is possible to determine that (ρ^*, θ^*) satisfies one of Eq. (15) or (16). For simplicity and tolerating the stochastic property of the measured and estimated quantities, θ is discretized as

$$\theta_j = (j - \frac{1}{2})\Delta\theta \qquad j = 1,2,..., M_\theta \qquad (19)$$

where $\Delta\theta$ indicates the step size representing the tolerance of θ and $M_\theta = \pi/\Delta\theta$. The sets of ρ_j corresponding to θ_j for Eqs. (15)-(18) are then defined. The difference of ρ_j under θ_j for the predicted states is defined as follow

$$\Delta\rho_j(n) = \left|\rho_j(n) - \rho_j(n-1)\right| \quad j = 1,2,...,M_\theta \qquad (20)$$

θ^* is determined from Eq. (19) by inspecting every θ_j which relates to minimum value of $\Delta\rho_j(n)$. Define

$$\Delta\rho_{i\theta^*}(n+1) = \left|\rho_{ij}(n+1) - \rho_j(n)\right|_{\theta=\theta^*} \quad i = 1,2,\cdots,N_o \quad j = 1,2,...,M_\theta \qquad (21)$$

$$\Delta\rho^c_{i\theta^*}(n+1) = \left|\rho^c_{ij}(n+1) - \rho_j(n)\right|_{\theta=\theta^*} \quad i = 1,2,\cdots,N_o \quad j = 1,2,...,M_\theta \qquad (22)$$

Let the set with N elements

$$\Delta\rho(n+1) = \{\Delta\rho_{1\theta^*}, \Delta\rho_{2\theta^*}, \cdots, \Delta\rho_{N_o\theta^*}, \Delta\rho^c_{1\theta^*}, \Delta\rho^c_{2\theta^*}, \cdots, \Delta\rho^c_{N_c\theta^*}\} \qquad (23)$$

Two sets of measurements, $\boldsymbol{Z}^*_{c1}(n+1)$ and $\boldsymbol{Z}^*_{c2}(n+1)$, corresponding to $\Delta\rho^*_{c1}(n+1)$ and $\Delta\rho^*_{c2}(n+1)$ with two smallest values in $\Delta\rho(n+1)$, are selected. $\boldsymbol{Z}^*_{c1}(n+1)$ and $\boldsymbol{Z}^*_{c2}(n+1)$ will be sent into the EKF with input estimation and MPDAF for trajectory estimation.

IV. EXTENDED KALMAN FILTER WITH INPUT ESTIMATION

The input estimation algorithm estimates unknown inputs in state equations from pseudo-residuals. The predicted and updated states vectors of the *i*-th candidate, $i = 1,2$, by the EKF from $t = n\Delta t$ to $t = (n+1)\Delta t$, $n = 0,1,2,...$, under known input vector $\boldsymbol{u}_{ci}(n)$ are given by, respectively, [4]

$$\hat{\boldsymbol{X}}_{ci}(n+1|n) = \phi(n)\hat{\boldsymbol{X}}^v(n|n) + \varphi_\Delta \boldsymbol{u}(n) \qquad (24)$$

$$\hat{\boldsymbol{X}}_{ci}(n+1|n+1) = \hat{\boldsymbol{X}}_{ci}(n+1|n) + \boldsymbol{K}_{ci}(n+1) \times [\boldsymbol{Z}^*_{ci}(n+1) - \hat{\boldsymbol{X}}_{ci}(n+1|n)] \qquad (25)$$

where $\varphi_\Delta = \varphi\Delta t$, $\boldsymbol{K}_{ci}(n+1)$ is the Kalman gain and

$$\phi(n) = \boldsymbol{I}_{6\times 6} + \left.\frac{\partial \boldsymbol{F}(\boldsymbol{X})}{\partial \boldsymbol{X}}\right|_{\boldsymbol{X}=\hat{\boldsymbol{X}}^v(n|n)} \Delta t$$

Let $\overline{\boldsymbol{X}}_{ci}(n+1|n+1)$ denote the updated states for the EKF with no input at $t = (n+1)\Delta t$. Let $\hat{\boldsymbol{X}}_{ci}(n+1) = \hat{\boldsymbol{X}}_{ci}(n+1|n+1)$ and $\overline{\boldsymbol{X}}_{ci}(n+1) = \overline{\boldsymbol{X}}_{ci}(n+1|n+1)$ for simplicity. Define

$$\boldsymbol{M}_{ci}(n+1) = [\boldsymbol{I} - \boldsymbol{K}_{ci}(n+1)]\phi(n) \qquad (26)$$

$$\boldsymbol{N}_{ci}(n+1) = [\boldsymbol{I} - \boldsymbol{K}_{ci}(n+1)]\varphi_\Delta \qquad (27)$$

Assume that the abrupt deterministic inputs, induced by model error, are applied during $k\Delta t \le t \le (k+s)\Delta t$,

$$\boldsymbol{u}_{ci} = \begin{cases} 0 & t < k\Delta t, t > (k+s)\Delta t \quad k,s > 0 \\ \boldsymbol{u}_{ci}(k+l) & k\Delta t \le t \le (k+s)\Delta t \quad l = 0,1,2,...,s \end{cases} \qquad (28)$$

where $\boldsymbol{u}_{ci}(k+l)$ is a constant vector over the sampling interval. Then, $\hat{\boldsymbol{X}}_{ci}(k) = \overline{\boldsymbol{X}}_{ci}(k)$ during $t \le k\Delta t$. The difference induced by the abrupt inputs between these two formations during $k\Delta t \le t \le (k+s)\Delta t$ can then be written as

$$\Delta\boldsymbol{X}_{ci}(k+l) = \hat{\boldsymbol{X}}_{ci}(k+l) - \overline{\boldsymbol{X}}_{ci}(k+l) = \boldsymbol{M}_{ci}(k+l)\Delta\boldsymbol{X}_{ci}(k+l-1) + \boldsymbol{N}_{ci}(k+l)\boldsymbol{u}_{ci}(k+l-1) \qquad (29)$$

Define the measurement residual for the EKF formation without and with inputs to be $\overline{\boldsymbol{Z}}_{ci}(k+l) = \boldsymbol{Z}^*_{ci}(k+l) - \overline{\boldsymbol{X}}_{ci}(k+l)$ and $\hat{\boldsymbol{Z}}_{ci}(k+l) = \boldsymbol{Z}^*_{ci}(k+l) - \hat{\boldsymbol{X}}_{ci}(k+l)$, respectively. The recursive least-squares input estimator can be derived as [4]

$$\hat{\boldsymbol{u}}_{ci}(k+l-1) = \hat{\boldsymbol{u}}_{ci}(k+l-2) + \boldsymbol{G}_{ci}(k+l) \times [\hat{\boldsymbol{Y}}_{ci}(k+l) - \boldsymbol{N}_{ci}(k+l)\hat{\boldsymbol{u}}_{ci}(k+l-2)] \qquad (30)$$

where

$$\hat{\boldsymbol{Y}}_{ci}(k+l) = \overline{\boldsymbol{Z}}_{ci}(k+l) - \boldsymbol{M}_{ci}(k+l)\Delta\hat{\boldsymbol{X}}_{ci}(k+l-1)$$

$$\Delta\hat{\boldsymbol{X}}_{ci}(k+l-1) = \boldsymbol{M}_{ci}(k+l)\Delta\hat{\boldsymbol{X}}_{ci}(k+l-2) + \boldsymbol{N}_{ci}(k+l)\hat{\boldsymbol{u}}_{ci}(k+l-2)$$

The gain $\boldsymbol{G}_{ci}(i)$ and variance of $\hat{\boldsymbol{u}}_{ci}(i)$, $\boldsymbol{V}_{ci}(i)$, are

$$\boldsymbol{G}_{ci}(k+l)=\boldsymbol{V}_{ci}(k+l-1)\boldsymbol{N}_{ci}(k+l)\times[\boldsymbol{R}+\boldsymbol{P}_{ci}(k+l|k+l-1)]^{-1} \quad (31)$$

$$\begin{aligned}\boldsymbol{V}_{ci}(k+l-1)=&\boldsymbol{V}_{ci}(k+l-2)-\boldsymbol{V}_{ci}(k+l-2)\boldsymbol{N}_{ci}(k+l)^T\\&\times\{\boldsymbol{N}_{ci}(k+l)\boldsymbol{V}_{ci}(k+l-2)\boldsymbol{N}_{ci}(k+l)^T\\&+[\boldsymbol{R}+\boldsymbol{P}_{ci}(k+l|k+l-1)]\}^{-1}\\&\times\boldsymbol{N}_{ci}(k+l)\boldsymbol{V}_{ci}(k+l-2)\end{aligned} \quad (32)$$

where $\boldsymbol{P}_{ci}(k+l|k+l-1)$ expresses the covariance matrix of the predicted states for the EKF with no input

$$\boldsymbol{P}_{ci}(k+l|k+l-1)=\phi(n)\boldsymbol{P}_{ci}(k+l-1|k+l-1)\phi(n)+\boldsymbol{Q}(\Delta t)^2$$

$$\boldsymbol{P}_{ci}(k+l|k+l)=[\boldsymbol{I}_{6\times6}-\boldsymbol{K}_{ci}(k+l)]\boldsymbol{P}_{ci}(k+l|k+l-1)$$

In Eq. (28), *k* and *s* respectively denote the starting and stopping indices of the system input, which can be obtained by testing. Two hypotheses, existence and absence of inputs, are set. Each normalized estimated input at time *k*+*l*-1 locates on the confidence interval [$-t_{st}$, t_{st}] if the first hypothesis is satisfied. Otherwise, the input is absent. The confidence interval can be obtained from the cumulative normal distribution table for a certain preset confidence level $1-\alpha$.

Once the input is estimated, the EKF is corrected with the estimated input at the same time. By incorporating the on-line input estimator into the EKF, the predicted and updated states at time interval $k\Delta t \le t \le (k+s)\Delta t$ are given by

$$\hat{\boldsymbol{X}}^{v}_{ci}(k+l|k+l-1)=\phi(k+l-1)\hat{\boldsymbol{X}}^{v}_{ci}(k+l-1|k+l-1)+\varphi_{\Delta}\hat{\boldsymbol{u}}_{ci}(k+l-1) \quad (33)$$

$$\hat{\boldsymbol{X}}^{v}_{ci}(k+l|k+l)=\hat{\boldsymbol{X}}^{v}_{ci}(k+l|k+l-1)+\boldsymbol{K}^{v}_{ci}(k+l)\times[\boldsymbol{Z}^{*}_{ci}(k+l)-\hat{\boldsymbol{X}}^{v}_{ci}(k+l|k+l-1)] \quad (34)$$

The Kalman gain becomes

$$\boldsymbol{K}^{v}_{ci}(k+l)=\boldsymbol{P}^{v}_{ci}(k+l|k+l-1)\times[\boldsymbol{P}^{v}_{ci}(k+l|k+l-1)+\boldsymbol{R}]^{-1} \quad (35)$$

with the covariance matrices at $k\Delta t \le t \le (k+s)\Delta t$ being

$$\begin{aligned}\boldsymbol{P}^{v}_{ci}(k+l|k+l-1)=&\boldsymbol{P}_{ci}(k+l|k+l-1)\\&+\phi(k+l-1)\boldsymbol{L}_{ci}(k+l)\phi^{T}(k+l-1)\\&+\varphi_{\Delta}\boldsymbol{V}_{ci}(k+l-1)\varphi^{T}_{\Delta}\end{aligned} \quad (36)$$

$$\boldsymbol{P}^{v}_{ci}(k+l|k+l)=[\boldsymbol{I}_{6\times6}-\boldsymbol{K}^{v}_{ci}(k+l)]\boldsymbol{P}^{v}_{ci}(k+l|k+l-1) \quad (37)$$

where

$$\boldsymbol{L}_{ci}(k+1)=0$$

$$\boldsymbol{L}_{ci}(k+2)=\boldsymbol{N}_{ci}(k+2)\boldsymbol{V}_{ci}(k)\boldsymbol{N}^{T}_{ci}(k+2)$$

$$\boldsymbol{L}_{ci}(k+l)=\boldsymbol{M}_{ci}(k+l-1)\boldsymbol{L}_{ci}(k+l-1)\boldsymbol{M}^{T}_{ci}(k+l-1)$$

V. MODIFIED PROBABILISTIC DATA ASSOCIATION FILTER

The MPDAF is designed to track the warhead between two objects separation from the RV in a clear environment [11]. The filter provides the combined predicted and updated states vectors weighted by the probability of originating from the target. The probabilities with respect to two objects are determined by examining the normalized innovations of two candidates selected by target acquisition.

Define the events to be

$$\theta_1(n+1)=\{\boldsymbol{Z}^{*}_{c1}(n+1) \text{ is the target-originated measurement}\} \quad (38)$$

$$\theta_2(n+1)=\{\boldsymbol{Z}^{*}_{c2}(n+1) \text{ is the target-originated measurement}\} \quad (39)$$

with association probabilities conditioned on all measurements from *t*=0 to *t*=(*n*+1)Δ*t*, $\boldsymbol{Z}^{n+1}$,

$$\beta_1(n+1)=\Pr\{\theta_1(n+1)|\boldsymbol{Z}^{n+1}\} \quad (40)$$

$$\beta_2(n+1)=\Pr\{\theta_2(n+1)|\boldsymbol{Z}^{n+1}\} \quad (41)$$

The association probabilities should satisfy

$$\beta_1(n+1)+\beta_2(n+1)=1 \quad (42)$$

Then we have the combined updated state

$$\hat{\boldsymbol{X}}^v(n+1|n+1)=\beta_1(n+1)\hat{\boldsymbol{X}}^v_{c1}(n+1|n+1)+\beta_2(n+1)\hat{\boldsymbol{X}}^v_{c2}(n+1|n+1) \quad (43)$$

The problem then focuses on the determination of β_i by means of $\boldsymbol{Z}^*_{c1}(n+1)$ and $\boldsymbol{Z}^*_{c2}(n+1)$.

As previously mentioned, warhead trajectory is closer to the original than of the body, debris, and clutter. The innovations of the warhead are smaller than of other objects if an accurate estimation method is adopted. The larger association probability should be assigned to an object whose innovation is the smaller one between two objects. Thus, the association probabilities of the *i*-th object is inversely proportional to length of the normalized innovation in position and is then defined as [11]

$$\beta_1(n+1)=\frac{e_2}{e_1+e_2} \quad (44)$$

$$\beta_2(n+1)=\frac{e_1}{e_1+e_2} \quad (45)$$

where $e_1$and e_2 are length of the normalized innovation in position. Substituting Eqs. (44) and (45) into Eq. (43) yields the combined updated state of the target in track at $t=(n+1)\Delta t$. This estimated trajectory should be close to warhead trajectory, such that the radar search pattern covers the warhead to maintain the track.

Figure 3 shows the mechanism of the proposed tracking algorithm scheme and the detailed steps are illustrated as follows.

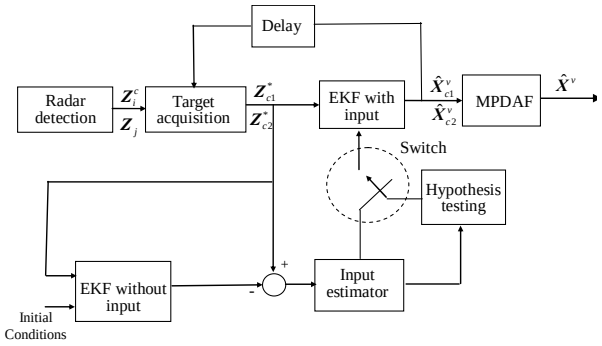

Fig. 3 Mechanism of the proposed tracking algorithm scheme.

Step 1 Computing $\rho(n\text{-}1)$ and $\rho(n)$ from Eqs. (17) and (18) based on two quantities, $(\hat{q}^v_u(n-1|n-1),\hat{q}^v_v(n-1|n-1))$ and $(\hat{q}^v_u(n|n),\hat{q}^v_v(n|n))$ in updated states, $\hat{\boldsymbol{X}}^v(n-1|n-1)$ and $\hat{\boldsymbol{X}}^v(n|n)$, respectively.

Step 2 Discretizing $\rho(n\text{-}1)$ and $\rho(n)$ as M_θ intervals following $\Delta\theta$ and θ_j defined in Eq. (19).

Step 3 Computing the difference between $\rho(n\text{-}1)$ and $\rho(n)$, $\Delta\rho_j(n)$, for each interval using Eq. (20).

Step 4 Determining θ^* from Eq. (20) by inspecting every θ_j that relates to minimum value of $\Delta\rho_j(n)$.

Step 5 Calculating $\Delta\rho_{\theta^*}(n+1)$ and $\Delta\rho^c_{i\theta^*}(n+1)$ from Eqs. (21) and (22) under θ^* for every measurement.

Step 6 Forming $\Delta\rho(n+1)$, Eq. (23), by $\Delta\rho_{\theta^*}(n+1)$ and $\Delta\rho^c_{i\theta^*}(n+1)$.

Step 7 Selecting two smallest values in $\Delta\rho(n+1)$, $\Delta\rho^*_{c1}(n+1)$ and $\Delta\rho^*_{c2}(n+1)$, and the corresponding measurements $\boldsymbol{Z}^*_{c1}(n+1)$ and $\boldsymbol{Z}^*_{c2}(n+1)$.

Step 8 Estimating input $\hat{\boldsymbol{u}}_{ci}(n+1)$ and state $\hat{\boldsymbol{X}}^v_{ci}(n+1|n+1)$ in Eqs. (30) and (34) using $\boldsymbol{Z}^*_{ci}(n+1)$, $i=1,2$.

Step 9 Calculating associate probabilities, $\beta_1(n+1)$ and $\beta_2(n+1)$, from Eqs. (44) and (45) and combined updated state $\hat{\boldsymbol{X}}^v(n+1|n+1)$ in Eq. (44).

Step 10 Letting n+1:=n+2 and returning to *Step* 1.

VI. SIMULATION ANALYSIS

The proposed tracking algorithm comprising the target acquisition algorithm, the EKF with input estimation and the MPDAF is assessed by simulation in this section. To show the importance of an accurate trajectory estimation method, simulation results for the proposed algorithm, Method I, are compared with those of obtained with the original EKF,

Method II. Performance is evaluated by inspecting the association probabilities for two selected objects and estimation error. The association probability assigned to the warhead should be greater than that assigned to another object that means the estimated warhead trajectory approaches to the true warhead trajectory. Estimation error with respect to (w.r.t.) the warhead, which is the difference between the estimated and the true warhead trajectories, should be low during tracking, thereby ensuring that the tracked target is a warhead but other objects. A high association probability and low estimation error relating for a warhead guarantee that the radar is tracking well.

The warhead, body, and debris trajectories are generated by Eqs. (7)-(9) along with four pieces of clutter, which are uniformly distributed within the same search pattern. The measurement noises are from the normal distributions. The number of clutter within a search pattern is normally Poisson distributed with the average number which is typically lower than 3 for filter analysis [9]. To demonstrate the tracking performance of the proposed method, the worst case with four pieces of clutter at each search in entire simulation is considered. Clutter position is generated within a search pattern centered on warhead location and radius

$$r_b = 6R_t(t)\sin(\theta_{bw}) \tag{46}$$

where $R_t(t)$ is the slant range to the warhead at time t and θ_{bw} is the beamwidth of the radar beam. For the radar being considered in the system, the beamwidth is θ_{bw}=1.2°. Two cases, non-maneuvering and maneuvering RV, with 50 Monte Carlo runs for each are considered as follows.

Consider an RV in the reentry phase with $C = 2500kg/m^2$ and initial values of $x(0) = 300m$, $y(0) = 300m$, $z(0) = 30500m$, $v(0) = 1500m/\sec$, $\gamma_1(0) = 65^o$, and $\gamma_2(0) = 15^o$. The RV separates into the warhead, body, and two pieces of debris with ballistic coefficients $C_1 = 2000kg/m^2$, $C_2 = 3000kg/m^2$ $C_3 = 3500kg/m^2$, and $C_4 = 4000kg/m^2$, respectively, at t_s=13 *seconds*. Figures 4-9 present the measured positions and velocities of the warhead, body, and debris, respectively. The RV body and two pieces of debris fall faster than the warhead. Figures 10-12 show four pieces of clutter locations in three axes spread around the warhead within r_b. The measured velocity in the X_R-Y_R plane is considered for the Hough transform. The step size, $\Delta\theta$, relates the tolerance of finding θ^* and $\Delta\rho(n+1)$. In this section, let $\Delta\theta = 5^\circ$. Let the confidence level 1-α to be 95% that is the confidence interval [-t_{st}, t_{st}]=[-1.96, 1.96]. The values of $\boldsymbol{R}$ and $\boldsymbol{Q}$ were taken $\boldsymbol{I}_{6\times6}$ both and the initial conditions of $\boldsymbol{V}(0)$ and $\boldsymbol{P}^v(0|0)$ were $500\boldsymbol{I}_{6\times6}$ both. The first measurement, $\boldsymbol{Z}(0)$ is taken as the initial state vector, $\hat{\boldsymbol{X}}^v(0|0)$ .The sampling period of the radar is set to Δt=0.25 *seconds*.

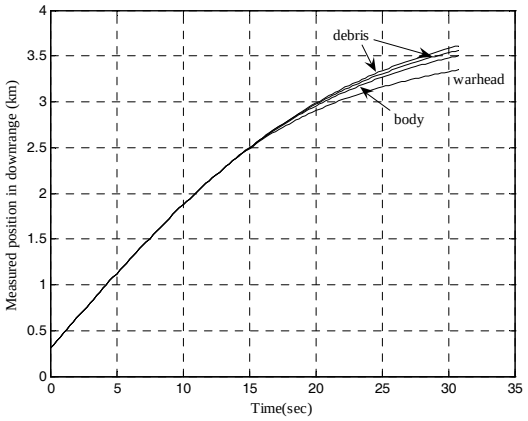

Fig. 4 Measured positions in X_R for the warhead, body and debris.

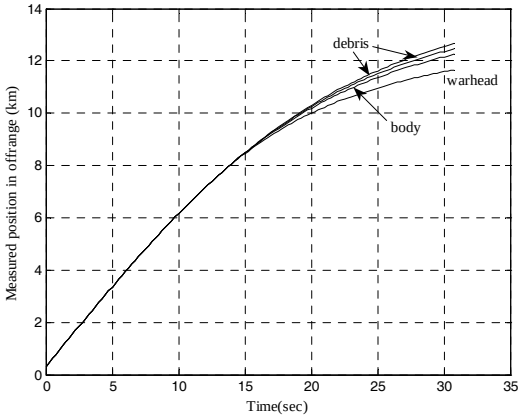

Fig. 5 Measured position in Y_R for the warhead, body and debris.

Figure 13 displays the association probabilities assigned to the warhead and

another object by Method I. The association probability assigned to the warhead reaches almost 1 in 7 *seconds* after separation that means the effects to the trajectory estimation by body, debris, or clutter, are reduced to almost zero. Figures 14 and 15 depict the estimation errors in position and velocity, respectively. Position estimation errors are lower than 20*m* and velocity estimation errors are within (20*m/sec*, -10*m/sec*). These results indicate that the warhead is tracked well. Figure 16 presents the association probability generated by Method II. The association probability assigned to the warhead gradually approaches to zero that the warhead is lost. Spikes in this figure indicate that clutter is involved and degrades the estimation. The estimation errors in position and velocity, Figs. 17 and 18, are also considerably larger than those obtained by Method I. Clearly, Method I is superior to Method II and tracks the warhead well.

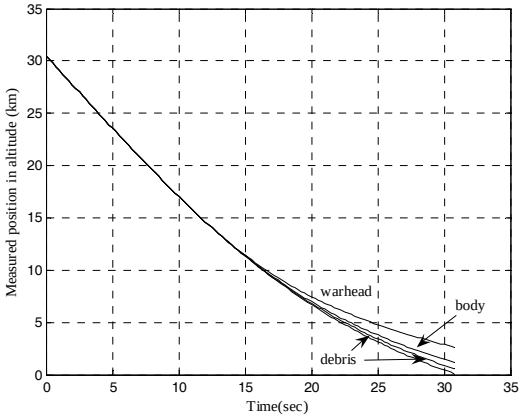

Fig. 6 Measured positions in Z_R for the warhead, body and debris.

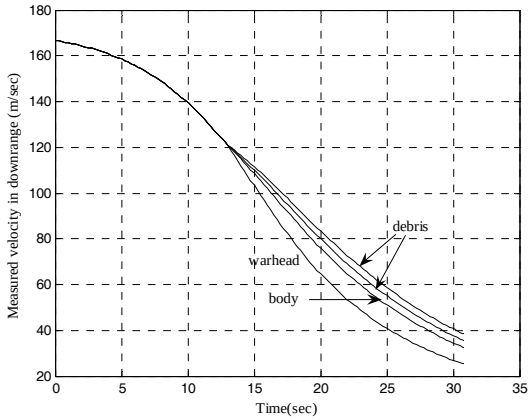

Fig. 7 Measured velocities in X_R for the warhead, body and debris.

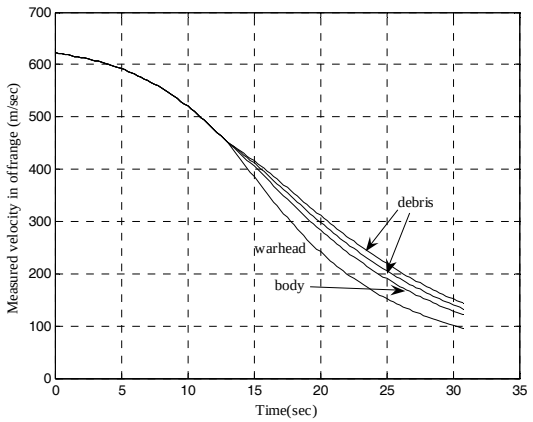

Fig. 8 Measured velocities in Y_R for the warhead, body and debris.

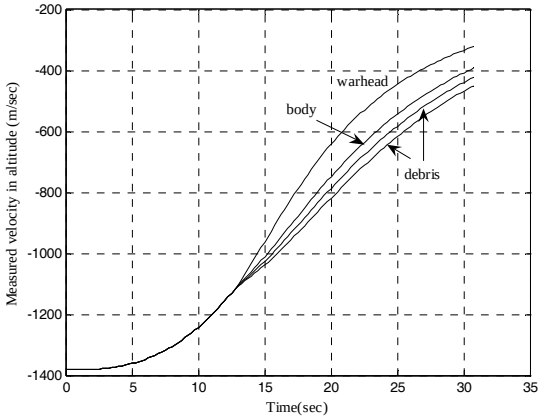

Fig. 9 Measured velocities in Z_R for the warhead, body and debris.

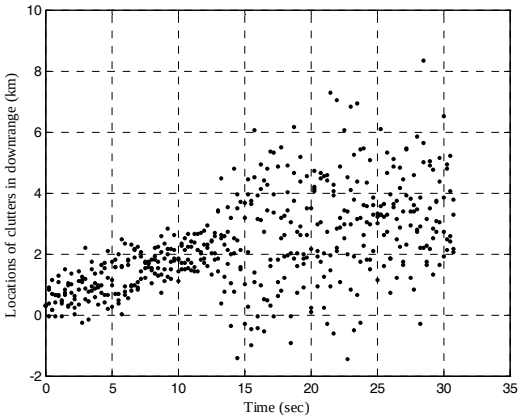

Fig. 10 Location of clutter in downrange.

Consider an RV to undertake a series of maneuver, $u_x=u_y=5G$ at $t=5 \sim 7$ *seconds* and $u_z=-5G$ at $t=7 \sim 9$ *seconds*, before separation. Figure 19 illustrates the assigned association probabilities assigned to the warhead and another object by Method I which is similar with

those obtained in non-maneuvering case. It ensures that the warhead will be tracked well after separation. The estimation error norms induced by Method I, Fig. 20, still keep lower than 30*m* in position and 30*m*/*sec* in velocity. Figure 21 demonstrates the assigned associate probabilities offered by Method II which has a slight difference as comparing with those obtained in non-maneuvering case. Figure 22 displays the estimation error norms which are much greater than those generated by Method I and make the radar to track another object but the warhead.

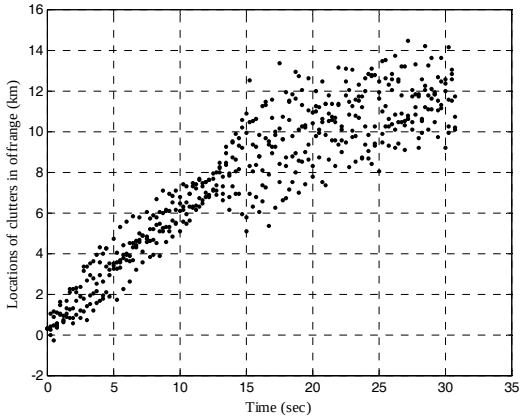

Fig. 11 Location of clutter in offrange.

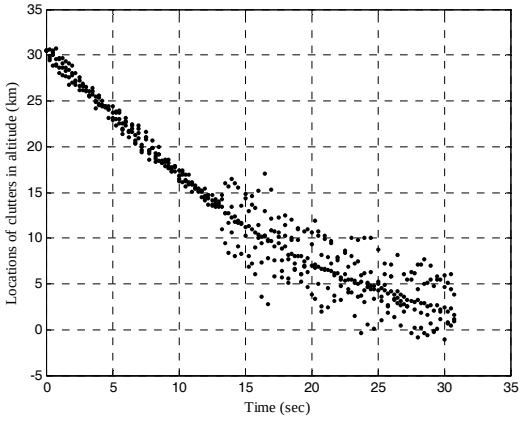

Fig. 12 Location of clutter in altitude.

In non-maneuvering and maneuvering cases, numbers of echo of the warhead, body, debris, and clutter being selected to be candidates by means of the target acquisition algorithm are given in Table 1. Method I provides a good clutter suppression performance that no clutter was chosen and body was totally rejected from tracking file in 8 *seconds* after separation for both cases. Nevertheless, several pieces of clutter and debris were selected by Method II that cause the warhead to be dropped in 4 *seconds* after splitting.

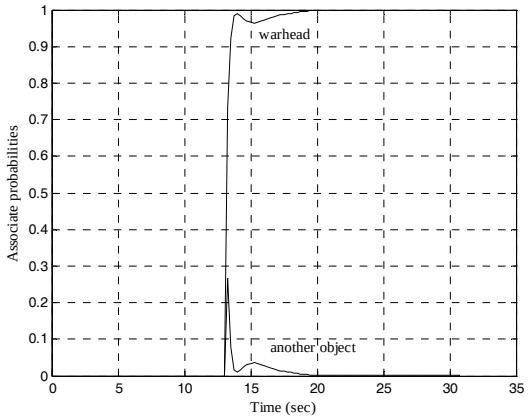

Fig. 13 Association probabilities assigned by Method I.

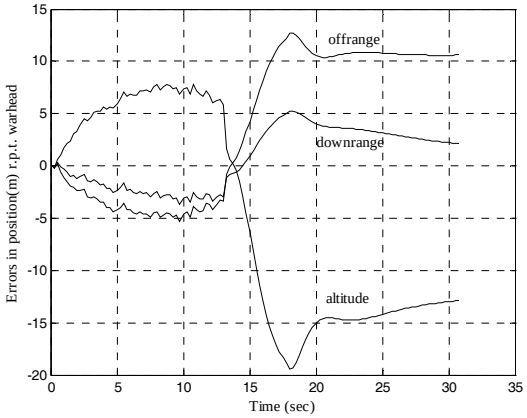

Fig. 14 Position estimation error Method I w.r.t. warhead.

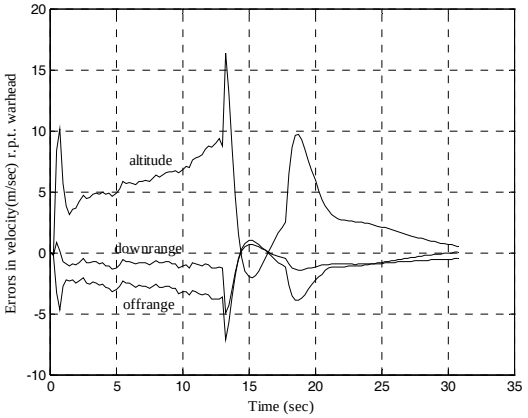

Fig. 15 Velocity estimation error Method I w.r.t. warhead.

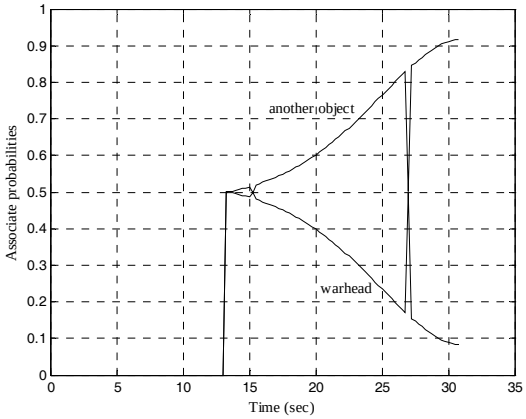

Fig. 16 Association probabilities assigned by Method II.

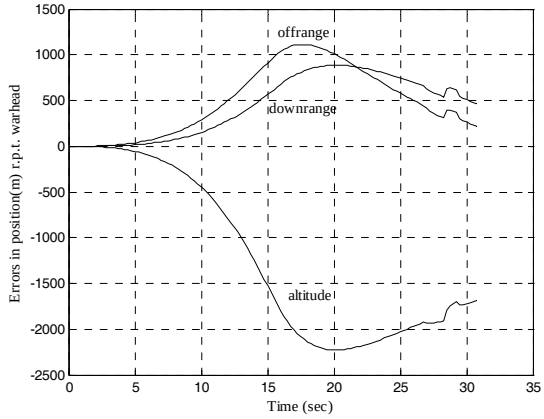

Fig. 17 Position estimation error of Method II w.r.t. warhead.

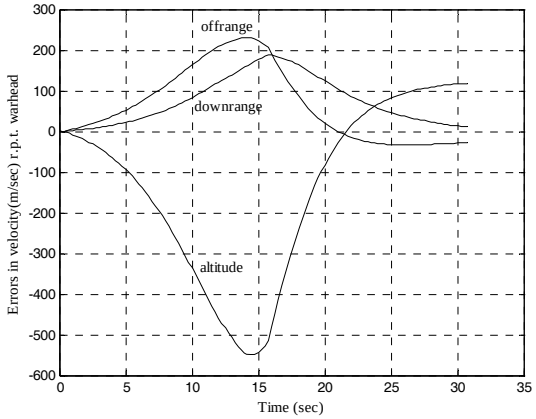

Fig. 18 Velocity estimation error of Method II w.r.t. warhead.

VII. CONCLUSIONS

This study presents an accurate method for tracking a non-maneuvering warhead among objects separated from an RV in cluttered environments. The proposed method composed of the novel target acquisition algorithm based on the HT, EKF with IE and MPDAF. The target acquisition algorithm chooses two candidates from detected objects and clutter. The EKF associated with input estimation resolves the model error problem and accurately estimates the trajectories of the RV and objects. The MPDAF predicts warhead trajectory using estimated trajectories of two candidates. The loop involving estimation and identification effectively tracks the warhead. Simulation results are used to assess the performance of the proposed algorithm by examining association probability and estimation errors to ensure good tracking performance. However, improving the algorithm for reducing the search pattern in order to save the radar resource is an important issue for future study. Although the maneuvering warhead is seldom mentioned, its tracking is still a big problem and should be investigated in the future.

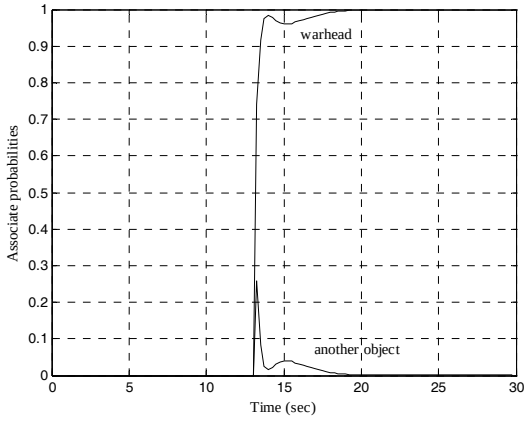

Fig. 19 Association probabilities assigned by Method I for the maneuvering RV.

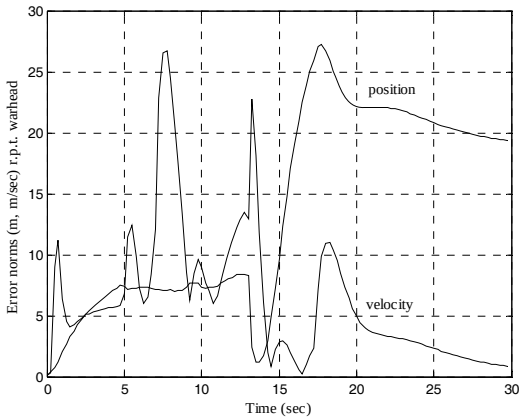

Fig. 20 Estimation error norms of Method I w.r.t. the warhead for the maneuvering RV.

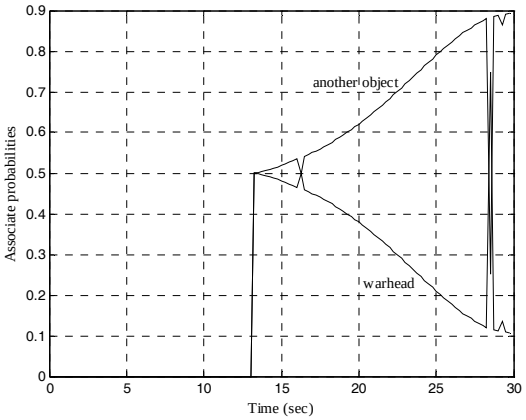

Fig. 21 Association probabilities assigned by Method II for the maneuvering RV.

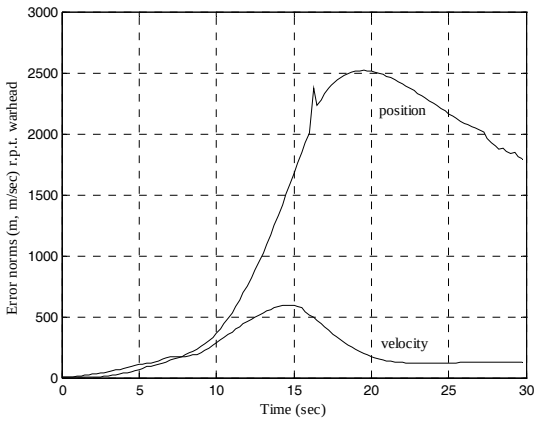

Fig. 22 Estimation error norms of Method II w.r.t. the warhead for the maneuvering RV.

Table 1 Numbers of echo being selected to be the first ($\boldsymbol{Z}_{c1}^{*}$) and second ($\boldsymbol{Z}_{c2}^{*}$) candidates in non-maneuvering (N. M.) and maneuvering (M.) cases.

		warhead		body		debris		clutter	
Cases	Methods	$\boldsymbol{Z}_{c1}^{*}$	$\boldsymbol{Z}_{c2}^{*}$	$\boldsymbol{Z}_{c1}^{*}$	$\boldsymbol{Z}_{c2}^{*}$	$\boldsymbol{Z}_{c1}^{*}$	$\boldsymbol{Z}_{c2}^{*}$	$\boldsymbol{Z}_{c1}^{*}$	$\boldsymbol{Z}_{c2}^{*}$
N.M.	I	72	0	0	72	0	0	0	0
	II	70	0	0	69	1	1	1	2
M.	I	68	0	0	68	0	0	0	0
	II	64	2	0	64	1	1	3	1

ACKNOWLEDGMENT

The authors would like to thank the National Science Council of the Republic of China, Taiwan for financially supporting this research under Contract No. NSC95 – 2221 –E – 234 - 004.

REFERENCES

[1] Edde, B., Radar principles, technology, applications, Prentice Hall , Inc. , 1993.

[2] Blackman, S. S., Multiple-target tracking with radar applications, Artech House, Inc. , 1986.

[3] Chen, J., Leung H., Lo, Litva, T., J., and Blanchette, M., "A modified probabilistic data association filter in a real clutter environment," IEEE Transactions on Aerospace and Electronic System, Vol. 32, No. 1, pp. 300-313, 1996.

[4] Lee, S. C. and Liu, C. Y., "Trajectory estimation of reentry vehicles by use of on-line input estimation," J. of Guidance, Control, and Dynamics, Vol. 22, pp. 808-815, 1999.

[5] Liu, C. Y., Wang, H. M., and Tuan, P. C., "Input estimation algorithms for reentry vehicle trajectory estimation," Defence Science Journal, Vol. 55, No. 4, pp. 361-375, 2005.

[6] Liu, C. Y., Liu, C. C., and Tuan, P. C., "Algorithm of impact point prediction for intercepting reentry vehicles," Defence Science Journal, Vol. 56, No. 2, pp.129-146, 2006.

[7] Bar-Shalom, Y. and Tse, E., "Tracking in a cluttered environment with probabilistic data association," Automatica, Vol. 11, pp. 451-460, 1975.

[8] Fortmann, T. E., Bar-Shalom, Y., and Scheffe, M., "Sonar tracking of multiple targets

using joint probabilistic data association", IEEE Journal of Oceanic Engineering, Vol. 8, No. 3, pp. 173-184, 1983.

[9] Bar-Shalom, Y. and Fortmann, T.E., Tracking and Data Association, Academic Press Inc. , 1988.

[10] Chen, B. and Tugnait, J. K., "Tracking of maneuvering targets in clutter using imm/jpda filtering and fixed-log smoothing," Automatica, Vol. 37, pp. 239-249, 2001.

[11] Liu, C. Y. and Sung, Y. M., "Clarifying warhead separation from the reentry vehicle using a novel tracking algorithm," International Journal of Control, Automation, and Systems, Vol. 4, No. 5, pp. 529-538, 2006.

[12] Siouris, G. M., Aerospace Avionics System: A Modern Synthesis, Academic Press Inc. , 1993.